International Journal of GEOMATE, Sep., 2025 Vol.29, Issue 133, pp.129-138
ISSN: 2186-2982 (P), 2186-2990 (O), Japan, DOI: https://doi.org/10.21660/2025.133.5047
Geotechnique, Construction Materials and Environment

SAFETY ENHANCEMENT OF ERODED GABION WALL USING OPTIMIZED MINI-PILES

*Edward Ngii[1] and Anafi Minmahddun[1]

[1]Department of Civil Engineering, Engineering Faculty, Halu Oleo University, 93232, Kendari, Indonesia

*Corresponding Author, Received: 14 May 2025, Revised: 06 July 2025, Accepted: 09 July 2025

ABSTRACT: Gabion walls are widely used for slope stabilization, particularly in hilly areas. However, these structures are vulnerable to failure mechanisms, such as sliding due to scouring, compromising their effectiveness. This study investigates the stability of the gabion wall reinforced with mini-piles to address erosion-induced failures, focusing on a case study along the Maligano road in North Buton Regency, Southeast Sulawesi, Indonesia. The research integrates field observations, soil investigations, and finite element modeling to analyze the causes of gabion wall failure and evaluate the effectiveness of mini-pile reinforcement. The study demonstrated that mini-pile reinforcement significantly improves stability. Various pile lengths were tested, showing that the safety factor (SF) increased with pile length. A 1-meter pile length achieved an SF of 1.17, while a 1.5-meter pile length met the required threshold of 1.53. A maximum SF of 2.32 was observed for a 3-meter pile length. The study concludes that mini-piles effectively enhance gabion wall stability by intercepting potential slip surfaces and increasing safety. Although effective erosion control and drainage are essential for managing runoff and preventing scouring, the primary contribution of this research is the practical application of mini-piles in improving slope stability in erosion-prone areas, offering valuable insights for safer infrastructure development in challenging terrains.

Keywords: Gabion wall, Mini-pile, SF, Scouring, Slope failure

1. INTRODUCTION

Gabion walls, constructed from wire mesh baskets filled with stones, serve as versatile structural supports in civil engineering applications. Their primary uses include preventing soil erosion, stabilizing slopes, and managing water flow in flood-prone areas [1–4]. These walls are highly valued for their flexibility, adaptability, and ease of construction, making them particularly suitable for diverse geological conditions and various construction scenarios. The simplicity of the construction process, along with the availability of materials such as galvanized wire mesh and locally sourced stones, contributes to their growing popularity, especially in cost-sensitive regions [5]. Moreover, the gabion wall's permeable nature allows it to reduce hydrostatic pressure effectively, thus lowering the risk of failure during periods of heavy rainfall or flooding [6]. Studies have demonstrated that gabion walls possess significant resilience against dynamic loads, including those generated by seismic activities, due to their inherent flexibility [7, 8]. This article explores gabion wall design, construction, and reinforcement, focusing on integrating advanced materials and methods to enhance their structural stability.

Despite their advantages, gabion walls are susceptible to various failure mechanisms, which underscore the necessity of meticulous design and construction practices. Failures often stem from insufficient bearing capacity analysis, leading to instability and deformation over time. External factors such as seismic activities pose additional risks that must be adequately accounted for in the design phase [9, 10]. Substandard construction practices, including poor site preparation and inadequate materials, further compromise the structural integrity of the gabion wall [5, 11]. Effective drainage is critical to the stability of gabion wall structures; inadequate drainage solutions can lead to increased hydrostatic pressure, particularly in regions with heavy rainfall, resulting in potential failures [12]. Environmental factors such as extreme weather conditions and seismic events also need to be considered to ensure the gabion wall's long-term stability and effectiveness [13–15]. Addressing these challenges requires a comprehensive approach incorporating design optimization and quality construction practices.

Recent research has focused on enhancing the stability of gabion walls through various design improvements, material innovations, and reinforcement techniques. One promising approach involves the use of advanced materials and optimized structural designs. For example, optimize wire hooks and bends in gabion retaining walls to maintain structural integrity [11]. Utilization of basalt fiber-reinforced (BFR) gabion, which demonstrated a 25.68% increase in safety factor (SF) compared to traditional designs, primarily due to the enhanced tensile strength of BFR materials that improves resistance to deformation under load [8]. Computational methods such as finite element

analysis have also optimized gabion wall designs. A slope stabilization system that combines gabion walls with geogrid reinforcements was explored, highlighting the effectiveness of this integrated approach in mitigating the adverse effects of rainfall on slope stability [16]. Field studies further validate the practical applications of these techniques, with a stabilization system combining a gabion-faced geogrid-reinforced retaining wall with embedded piles, as demonstrated around Victoria, Australia [17]. Additionally, alternative filling materials, such as recycled construction and demolition waste, have been investigated as a sustainable and cost-effective option for gabion wall construction, with comparable performance to traditional materials [18]. These advancements collectively contribute to the enhanced stability and functionality of gabion walls in various civil engineering applications.

Integrating gabion walls with pile or mini-pile reinforcements presents a robust solution for enhancing slope stability, as piles of certain depths and strategic placements can significantly improve stability [19–21]. The behavior of slopes with embedded piles under various load conditions was investigated using the finite element method. The results indicate that the piles contributed up to a 42.9% increase in stability [22]. A slope stabilization system combining gabion walls with geogrid-reinforced retaining walls and piles was studied using three-dimensional finite element methods (FEM), demonstrating substantial improvements in slope SF, particularly under heavy rainfall conditions. The results reveal that this integrated approach can improve stability by up to 41.2% [16]. The integration of gabion with concrete piles at various slope angles was explored, highlighting that this combination can increase the SF from 1.11 to 2.58 [23].

Building on insights from previous literature [23], which simulated gabion-mini pile reinforcement in flat areas without considering scouring effects, this study proposes an advanced approach tailored to the unique challenges of hilly, erosion-prone regions. Previous research, while valuable, did not address critical issues such as scouring and the complex topography found in areas with steep slopes. To fill this gap, the present study simulates the placement of gabion-mini pile reinforcement, specifically in sloped areas impacted by scouring conditions frequently encountered on road slopes in hilly regions of Indonesia.

2. RESEARCH SIGNIFICANCE

This study introduces a novel hybrid reinforcement approach by integrating mini-piles with gabion walls to counteract erosion-induced slope failures, a critical yet underexplored issue in Indonesia's rainfall-prone hilly regions. Unlike previous studies that neglect scouring effects, this research applies finite element modeling to realistically simulate failure scenarios and assess the influence of pile length on stability. The originality lies in addressing the synergistic role of scouring and reinforcement within slope protection systems. By offering a cost-effective and scalable design, the findings contribute directly to geotechnical engineering practices and inform safer, more resilient infrastructure planning in erosion-vulnerable environments.

3. RESEARCH METHOD

This research focuses on a gabion wall failure along the Maligano road section in North Buton Regency, Southeast Sulawesi, Indonesia. This road is a crucial access route connecting the provincial capital to the North Buton Regency. The area experiences a tropical climate with an average annual rainfall of 2,286 mm, humidity around 80%, and temperatures ranging from 22°C to 34°C. The hilly terrain, especially at elevations around 50 meters above sea level with slopes of approximately 40% [24], often leads to slope stability issues during the cut-and-fill process required to meet alignment specifications in the road preservation process at sta. 8+200 gabion wall was used as embankment reinforcement to widen the road. These gabion walls failed over time, particularly during the rainy season, causing part of the road to collapse, as seen in Figure 1.

Fig.1 Maligano road section experiences a slope failure.

3.1 Site Observation and Topographic Survey

The initial stage of the analysis is to conduct site observation, including collecting, analyzing, and interpreting data on the physical conditions in the landslide area. This process aims to comprehensively understand the factors that influence slope stability. During this phase, an initial

field visit is conducted to observe the current site conditions and identify any visible signs of instability. Visual inspections are carried out, and observations of surface features like rock outcrops, soil profiles, and drainage patterns are recorded. Photographic documentation captures the site's current state, and preliminary soil or rock samples may be collected for further laboratory analysis.

The Topographic Survey is planned based on the observation findings, focusing on critical areas such as steep slopes, drainage paths, and other features essential to slope stability. The topographic conditions of the research location are obtained by combining Digital Elevation Model (DEM) data from the Indonesian Geoportal [25] with direct field measurements using polygon and tachymetry methods with total station equipment to establish a vertical and horizontal framework [26]. Topographic information is crucial because it is one of the factors that can significantly influence slope stability [27–29]. These techniques are used to obtain precise terrain measurements, which are then used to generate contour maps and cross-sections. These maps accurately represent the site's topography, highlighting important features like the slope's crest, toe, and faces.

3.2 Soil Investigations

Another factor that greatly influences slope stability is soil properties, as differences in soil type and stratigraphic conditions can greatly influence slope stability [30–32]. This research uses a combination of field and laboratory testing that refers to the Indonesian code (SNI) to obtain soil type information at the study site. Field soil investigations were carried out using a cone penetration test (CPT) [33] and a hand-boring (HB) [34] around the slope failure area. The Cone Penetration Tests (CPTs) were strategically placed along the cross-section of the slope failure location to obtain detailed information about the soil type and stratigraphy of the slope. This information is crucial for understanding the subsurface conditions and assessing the slope's stability. The CPT results are used to determine the soil behavior type (SBT), which is derived from the relationship between cone resistance (qc) and friction ratio (fr) as plotted on the Robertson chart [35]. This chart classifies soils based on their mechanical behavior, allowing for a more precise understanding of their characteristics. By identifying the soil type, the stiffness of the soil can be estimated using the qc value, with correlations proposed by Look [36]. Soil stiffness is a critical factor in slope stability analysis because it influences the soil's ability to resist deformation under load, directly impacting the estimation of soil parameter values.

Unlike the Cone Penetration Test (CPT), which was more broadly applied across the slope, many hand-boring tests were concentrated at the toe of the gabion wall. This focus was due to the recognition that the slope failure was relatively shallow, with a depth approximately 2 meters, classifying it as a shallow failure [37]. These tests reached a depth of 2 meters, where soil samples were collected for laboratory analysis. The laboratory tests followed Indonesian National Standards (SNI), including grain-size analysis [38], density [39], specific gravity [40], water content [41], Atterberg limits [42, 43], and direct shear tests [44].

3.3 Slope Stability Analysis

The initial stage of the stability analysis involves the creation of a detailed slope model. This model uses a 2D finite element approach with plane strain idealization, ensuring the analysis accurately reflects the site's conditions. The soil stratigraphy for the model is created based on the classification results from the CPT and correlated with laboratory test outcomes.

Once the slope model is established, the next step is to input the relevant soil parameters into the model. These parameters include unit weight (γ), cohesion (c), internal friction angle (ϕ), elastic modulus (E), and Poisson's ratio (υ). These values are derived from laboratory test results and correlated with CPT data using established methods [36], while also considering real field conditions, ensuring the analysis is accurate and relevant.

The analysis uses the Mohr-Coulomb failure criteria, a widely accepted model for evaluating soil and rock failure [45–47]. The study is performed under several scenarios to assess the slope's behavior in different conditions, as seen in Table 1.

Table 1. Types of slope stability analysis

Type of analysis	Purpose of analysis	Remarks
End of Gabion wall construction analysis	Determine the initial SF	-
Slope stability analysis of gabion wall with scouring	Determining changes in SF due to erosion	-
Slope stability of gabion wall with pile reinforcement	Evaluation of the effect of pile depth on slope stability	Pile length: 1 m, 1.5 m, 2 m, 2.5 m and 3 m.

Each scenario helps understand the slope's behavior under various conditions and guides the design of appropriate mitigation measures. By combining detailed site observation, thorough soil investigations, and advanced modeling techniques,

this methodology provides a comprehensive assessment of slope stability and the effectiveness of reinforcement strategies. SF analysis was conducted using the shear strength reduction (SSR) method hat. This method systematically reduces the shear strength envelope of material by a factor of safety and computes FEM models of the slope until deformations are unacceptably large or solutions do not converge [48]. The application of SSR has been validated through various studies, demonstrating its effectiveness in different geological contexts [49].

4. RESULTS AND DISCUSSION

4.1 Site Observation and Topographic Survey

The topographic analysis reveals that the failure occurred in an inclined area, characterized by a hill on the left side and a ravine on the right, as depicted in Figure 2. The slope's history indicates that the right side, which eventually collapsed, was a former road embankment created during a widening process. This embankment became particularly vulnerable during heavy rainfall, which triggered the sliding of a gabion wall and caused a significant portion of the road to collapse. The actual conditions after the gabion wall failure were closely observed during the site visits. A critical issue identified was the absence of a drainage channel on the right side of the road, which allowed rainwater to flow uncontrollably along the slope's contour. This water flow pattern was carefully traced from the top side (Point A) down to Point B and then turning towards Point C, which leads directly to the toe of the gabion wall, as seen in Figure 2. The lower elevation at the toe of the gabion wall caused most of the water to accumulate in this area. The installation of the gabion wall altered the natural flow of water, which would have normally followed the road but was instead redirected towards the toe of the gabion wall. The elevation difference increased the speed of runoff, which intensified erosion at the slope's surface and led to the loss of passive earth pressure at the gabion wall toe.

There are three common types of retaining structure failures: bearing capacity failure, indicated by excessive settlement; overturning failure, where the structure tips over; and sliding failure, where the structure shifts horizontally. In this case, the failure mode of the gabion wall was found to be sliding failure. This conclusion was drawn from the observation that there was no excessive settlement or overturning of the gabion wall in the field; instead, the bottom of the gabion wall had shifted, as illustrated in Figure 1. Additionally, the stone filling within the gabion wire remained largely intact, with the wire being 90% in good condition. This observation found that the failure was not due to the gabion wire breaking under excessive stress but rather due to the sliding of the entire structure.

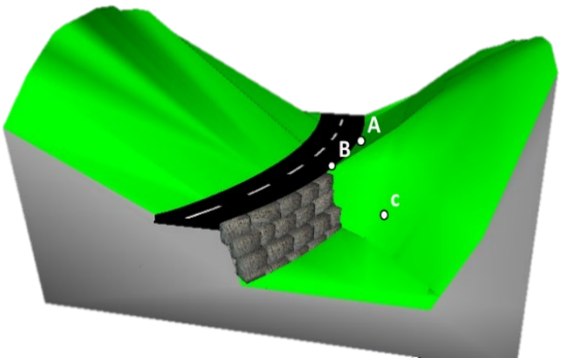

Fig.2 Theoretical gabion wall position

4.2 Result of Soil Investigations

Figure 3 and Table 2 present the CPT test results and soil classification. Figure 3 illustrates the CPT testing results at points 1 to 4 along the slope. Point 1 is located on the left side of the road, while points 2 to 4 are where the gabion wall collapsed. The test results reveal that hard soil, characterized by a qc value greater than 150 kg/cm², is present at depths of 3 to 5 meters. This hard soil layer provides a baseline for understanding the underlying stratigraphy and the transition between different soil types.

Table 2 provides the soil classification results, showing that the soil layer immediately above the bedrock behaves as silty sand with a very loose to lose density. Silty sand is a mixture of coarse-grained and fine-grained particles [50], with the proportion of fine grains significantly affecting its strength. When the fine grain content is less than 25%, it fills the voids between the coarse grains, increasing the soil's overall strength. The strength of silty sand is also influenced by its relative density, with denser soils exhibiting greater shear strength [51].

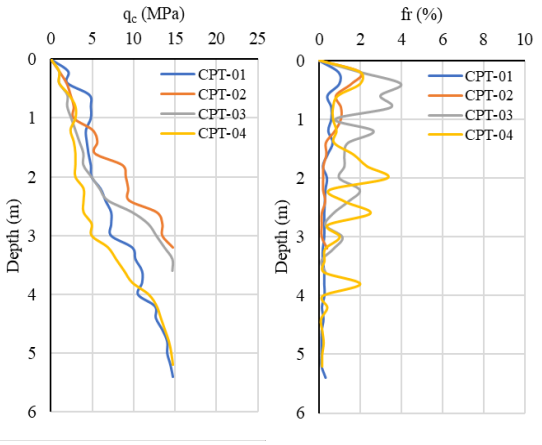

Fig.3 CPT test results

Table 2. Soil classification based on CPT

CPT-01		CPT-02	
Depth (m)	SBT	Depth (m)	SBT
0 – 0.4	5	0 – 0.4	4
0.4 – 5.4	6	0.4 – 1.2	5
		1.2 – 3.2	6
CPT-03		CPT-04	
Depth (m)	SBT	Depth (m)	SBT
0 - 0.8	4	0 – 0.4	4
0.8 – 2.4	5	0.4 – 2.6	5
2.4 – 3.6	6	2.6 – 5.2	6

Classification [35]:
4 = Clayey silt and silty clay; 5 = Silty sand and sandy silt; 6 = Clean sand to silty sand

However, slopes with silty sand can become unstable when the pore spaces between particles change, particularly due to wetting. Increased moisture content can reduce the soil's shear strength by increasing pore pressure, possibly leading to slope instability. Additionally, the interface between two soil layers with different properties, such as density or stiffness, can become a potential slip surface, where slope failure is more likely to initiate [52].

The laboratory test results for the soil samples obtained using hand-boring are listed in Table 3. According to the Unified Soil Classification System (USCS) [53], the soil was classified as silty sand (SM), a mixture of fine and coarse particles that plays a significant role in the slope's behavior. The laboratory analysis of the hand-bored soil samples revealed several key soil parameters crucial for assessing slope stability. The saturated unit weight of the soil was found to be between 16.7 and 17.4 kN/m³, slightly lower than the typical range for sandy soils (18 to 22 kN/m³), which suggests an increased potential for sliding, especially in retaining structures like gabion wall, where soil weight plays a significant role in stability [54].

The grain size distribution analysis showed that the soil was predominantly sandy, with particle sizes smaller than 4.75 mm. This fine grain size is particularly susceptible to erosion, with grains in the 0.2 to 0.6 mm range being highly prone to erosion [55]. The plasticity value only affects sandy soil a little because this parameter affects fine-grained soil (clay and silt) more. The shear strength tests revealed that the friction angle of the soil varied between 20° and 27°, which is still within the typical range for granular soils [36]. However, the presence of fine grain content reduces the soil's shear strength, as indicated by previous studies [56].

The soil investigation identified erosion at the gabion wall foundation as the main failure trigger. The silty sand at the foundation is highly susceptible to erosion, especially on a steep slope with increased surface runoff speed. The placement of the gabion wall on such a slope exacerbated this risk, leading to significant water scouring around the gabion wall base. This erosion weakened the foundation, ultimately causing the gabion wall to fail.

Table 3. Laboratory test results

Description	Unit	HB-01	HB-02	HB-03	HB-04
Specific gravity (Gs)	-	2.61	2.64	2.63	2.61
Unit weight					
- Moist (γ_b)	kN/m^3	16.1	13.8	14.6	13.6
- Saturated (γ_{sat})	kN/m^3	17.4	17.1	16.9	15.7
Sieve analysis					
- Pass #no. 4 (4.75 mm)	%	96.9	84.6	81.3	85.4
- Pass #no. 200 (0.075 mm)	%	13.5	14.2	15.4	14.8
Atterberg Limits					
- Liquid limit	%	21,95	19.86	23.11	25.12
- Plastic limit	%	20.57	17.34	20.86	22.01
- Plasticity index	%	1.38	2.51	2.25	3.11
Water content	%	31.32	17.97	27.20	32.04
Direct shear test					
- Cohesion (c)	kPa	4.1	2.4	2.2	2.8
- Friction angle (ϕ)	(°)	27.73	23.30	20.66	21.24

4.3 Slope Stability Analysis

The soil stratigraphy at the gabion wall location is illustrated in Figure 4a, where the soil is categorized into three distinct layers: a loose sand layer at the surface, followed by a medium dense layer, and finally, a dense sand layer serving as the bedrock. Based on the soil stratification, an analysis model was conducted, as seen in Figure 4b. The slope model was constructed using a rectangular mesh grid consisting of 100,000 mesh elements, allowing for a detailed analysis of slope stability.

The next stage involves inputting the parameter values for each soil layer. The shear strength parameters of the loose sand layer, which forms the gabion wall foundation, were obtained from the laboratory test results. The deformation parameters were determined through correlation with the CPT data. For the medium-dense and dense sand layers, both shear strength and deformation parameters were derived from CPT data correlation. However, the shear strength obtained from the CPT data correlation does not account for mixtures of coarse and fine-grain soil, such as silty sand. In this correlation, when the soil is dominated by sand, the parameters are limited to the internal friction angle and cohesion, with cohesion considered zero.

In contrast, silty sand contains a fine-grain fraction that contributes to the cohesion value. Therefore, the foundation soil parameters, which are crucial for controlling slope failure (as landslides tend to occur very shallowly), were selected from the results of direct shear tests, as they provide values for both the internal friction angle and

cohesion. The input parameters used in the analysis are listed in Table 4.

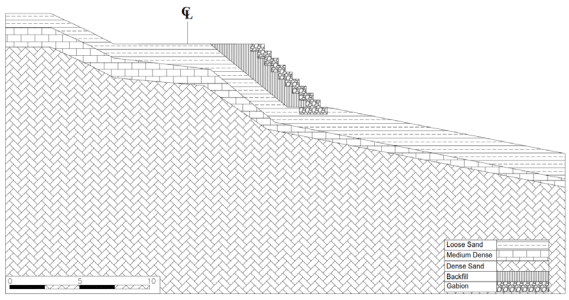

(a)

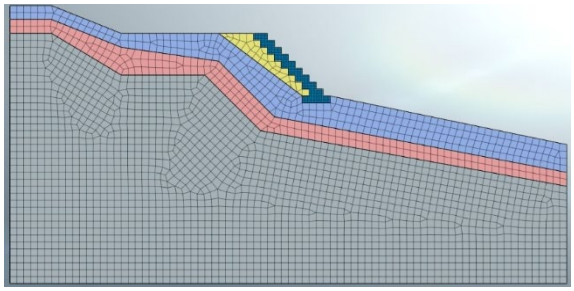

(b)

Fig. 4 (a) Stratigraphy and (b) Slope model

Table 4. Soil properties

Material	Loose sand	Medium dense	Dense sand	Backfill	Gabion
Model	M-C	M-C	M-C	M-C	L-E
γ (kN/m^3)	14	16	18	16	22
c (kPa)	2.2	0	0	12	-
φ (°)	20.66	30	35	23	-
E (kPa)	7×10^3	12×10^3	25×10^3	7.5×10^3	1×10^5
υ	0.33	0.33	0.33	0.33	0.2

Note: M-C = Mohr Coulumb; L-E = Linear elastic

4.3.1 End of gabion wall construction analysis

The slope analysis at the end of the construction period revealed that the slope's SF was 1.21, as shown in Figure 5. This value falls short of the SF criteria stipulated by the Indonesian Code in Geotechnical Design Requirements, which mandates a minimum slope SF of 1.5 [57]. Despite not meeting the required SF, the slope remained safe at the end of the construction period because its resistance was 1.2 times greater than the forces driving the slope to fail.

4.3.2 Slope stability analysis of gabion wall with scouring

The scouring depth was not calculated using empirical or analytical scour prediction equations. Instead, a simplified simulation method was adopted in the numerical model by artificially removing the soil mass in front of and below the gabion wall toe to represent the potential effects of scour. This approach assumes that erosion causes a loss of passive resistance at the toe, a condition commonly observed in field cases where concentrated water flow or prolonged rainfall leads to toe undermining.

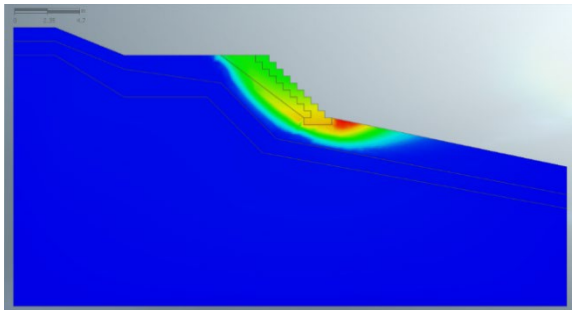

Fig. 5 SF after gabion wall construction

The analysis showed that, under this simulated scoured condition, the slope's factor of safety decreased to 1.08. Additionally, the critical slip surface was found to deepen, reaching approximately 1.3 m below the base of the gabion wall (Figure 6). This result highlights how scouring can destabilize the slope by promoting deeper failure mechanisms and reducing resisting forces. The 10.74% reduction in the SF is particularly concerning for slopes already in marginal stability conditions, as is the case in the study area.

Recent studies have highlighted the importance of understanding the scouring mechanisms of slope stability. A similarity model test examining the rainfall scouring mechanism of high-speed railway subgrade slopes, reveals that factors such as flow velocity and particle size play crucial roles in erosion [58]. This research underscores the need for quantitative analyses to characterize scouring erosion laws, which can inform the design and maintenance of slopes in railway engineering. Further investigation into coarse-grained soils has also shown that rainfall can directly dislodge soil particles, leading to significant erosion and slope destabilization [59].

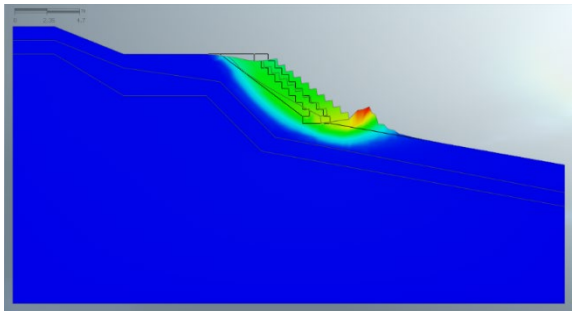

Fig. 6 SF of slopes with scouring

In Figure 6, the gabion wall deformation pattern shows the occurrence of sliding failure, similar to the field conditions. In addition, a slip surface depth

of <2 m also demonstrates similarities with actual conditions in the field. Of course, the analysis results will not match the exact conditions in the field due to simplifications in the model geometry and analysis parameters. However, the similarity of the slope failure patterns in the analysis results and the actual conditions in the field can validate the analysis results in this paper.

4.3.3 Slope stability of gabion wall with pile reinforcement

Based on field observations and analysis, the gabion wall failed due to sliding, primarily caused by the loss of passive pressure from scouring at the gabion's toe. To address this issue and enhance the stability of the gabion wall, mini piles with various depths were simulated to determine the minimum depth needed to be installed to prevent the gabion wall from collapsing due to scouring and unfavorable placement. The result of the stability analysis can be seen in Figure 7.

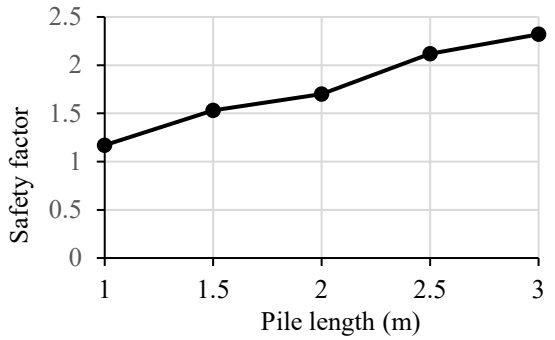

Fig. 7 SF of the slope with various pile lengths

The chart demonstrates how the SF (SF) increases with pile length, showing the effectiveness of pile reinforcement in enhancing slope stability. Starting with a pile length of 1 meter, the SF is 1.17, indicating a slight increase in strength compared to a scenario without piles. However, this value falls short of the minimum SF requirement of 1.50, meaning the slope remains marginally stable and prone to potential failure.

When the pile length increases to 1.5 meters, the SF rises significantly to 1.53, surpassing the required stability threshold. This considerable improvement occurs because the piles penetrate the critical slip plane, reinforcing the slope's weakest point and ensuring greater safety. As the pile length increases further, the SF continues to improve. At 2 meters, the SF reaches 1.70, further enhancing stability. At 2.5 meters, the SF jumps to 2.12, showing that the piles provide even greater resistance against slope failure. Finally, at a pile length of 3 meters, the SF reaches 2.32, representing the highest slope stability level observed in the chart.

It is important to note that while the increase in SF is significant up to a depth of 1.5 meters, further pile length increases result in a more moderate improvement. After the pile passes through the critical slip plane and reaches denser soil layers, the increase in the SF is less substantial. Nevertheless, each increment in pile length beyond 1.5 meters still contributes positively to overall slope stability, ensuring a higher safety margin against failure.

5. CONCLUSION

The study on enhancing gabion wall stability through mini-pile reinforcement, focusing on the case of erosion-induced failure along the Maligano road in North Buton Regency, Southeast Sulawesi, Indonesia, provides crucial insights into effective slope stabilization strategies in erosion-prone hilly terrains. The research reveals that the gabion wall failed primarily due to sliding caused by scouring at the base. This scouring, driven by uncontrolled runoff during heavy rainfall, led to significant erosion and a loss of passive earth pressure, resulting in instability. Observations confirmed that the failure mode was sliding rather than overturning or bearing capacity failure, as evidenced by the intact gabion wire and stone filling condition.

The soil at the failure site was identified as silty sand, which exhibited low shear strength and high susceptibility to erosion. Increased moisture content further compromised soil stability by elevating pore pressure and reducing shear strength. Initial slope stability analysis, conducted without reinforcement, revealed an SF (SF) of 1.21, below the required minimum of 1.50, indicating that the slope was marginally stable.

The integration of mini-piles was found to improve gabion wall stability significantly. Testing various pile lengths demonstrated that the SF increased with pile length. Specifically, a pile length of 1 meter yielded an SF of 1.17, while a height of 1.5 meters increased it to 1.53, meeting the required stability threshold. Further increases in pile length enhanced stability, with a maximum SF of 2.32 observed at 3 meters.

Overall, the study highlights the effectiveness of mini-pile reinforcement in enhancing slope stability and provides valuable insights into designing practical and reliable stabilization measures. While effective erosion control and drainage are important considerations for managing runoff and preventing scouring, this research focuses on the benefits of mini-piles for improving gabion wall stability in challenging, erosion-prone areas.

6. ACKNOWLEDGMENTS

The authors would like to gratefully acknowledge the Department of Water Resources and Highways Southeast Sulawesi Province,

Indonesia, for supporting funding for this research. The researchers also highly appreciate the support of the Soil Mechanics Laboratory of the Faculty of Engineering, Halu Oleo University.

7. REFERENCES

[1] Singh A. K., Dave M., Salvi R., Juneja, A., An Experimental Investigation into the Use of Three-Stepped Gabion Wall for Coastal Protection Works Using Acoustic Doppler Velocimeter, International Journal of Geosynthetics and Ground Engineering, 10(1), 2024, pp. 1–9. https://doi.org/10.1007/s40891-023-00510-6.

[2] Albaji M., Ershadian B., Nejad A. N., Mohammadi E., Dashtaki S. G., Determination of water erosion in Kowsar catchment area and evaluation of Gabion structures in its control, Environmental Earth Science, 79(22), 2020, p. 1-12. https://doi.org/10.1007/s12665-020-09248-0.

[3] Cho M. T. T., Chueasamat A., Hori T., Saito H., and Kohgo Y., Effectiveness of filter gabions against slope failure due to heavy rainfall, Soils Foundation, 61(2), 2021, pp. 480–495. https://doi.org/10.1016/j.sandf.2021.01.010.

[4] Liu J., Tan J., Zhang S., Zhong C., Lv L., Tara A., Suitability Assessment of Small Dams' Location as Nature-Based Solutions to Reduce Flood Risk in Mataniko Catchment, Honiara, Solomon Islands, Sustainability, 15(4), 2023, pp. 1–20. https://doi.org/10.3390/su15043313.

[5] Chikute G., Sonar I., Investigation of Gabion Wall Failures and Recommendations, in International Conference on Advances in Civil Engineering, vol 172, 2022, pp. 569–579. https://doi.org/10.1007/978-981-16-4396-5_49

[6] Cai X., Zhang S., Li S., Xu H., Zhu C., Liu X., Dynamic Characteristics of Reinforced Soil Retaining Wall With Composite Gabion Based on Time Domain Identification Method, Sustainability, 14(23), 2022, pp. 1-16. https://doi.org/10.3390/su142316321.

[7] Nakazawa H., Ishizawa T., Danjo T., Onoue Y., Suetsugu D., Hara T., Model Tests on the Stability of Retaining Walls with Gabions Under Earthquake and Rainfall Conditions, in International Conference on Protection of Historical Constructions, 2022, pp. 56–67. https://doi.org/10.1007/978-3-030-90788-4_5.

[8] Dai J., Xu X., Yang H., Su C., Ye N., Safety Risk Analysis of a New Design of Basalt Fiber Gabion Slope Based on Improved 3D Discrete Element Method and Monitoring Data, Sensors, 22(10), 2022, pp. 1-19. https://doi.org/10.3390/s22103645.

[9] Zhang H., Liu G., Wang Q., Yan Z., Xu G., Experimental Study on the Failure Mechanics of Gabion Elements Considering Multiple Factors, Geotechnical and Geological Engineering, Vol. 42, 2024, pp. 7085-7107. https://doi.org/10.1007/s10706-024-02916-z.

[10] Hanafi, Putra H. G., Andriani, Sliding failure analysis of a gabion retaining wall at km 31+800 of Lubuk Selasih-Padang city border highway, Indonesia, E3S Web Conference, Vol. 156, 2020, pp. 3–10. https://doi.org/10.1051/e3sconf/202015602005.

[11] Cajka R., Burkovis K., Neuwirthova Z., Mynarcik P., Bujdos D., Experimental Measurement Of The Load-Bearing Capacity Of Wire Hooks And Bends Used In Gabion Retaining Walls, International Journal of GEOMATE, 25(111), 2023, pp. 170–176. https://doi.org/10.21660/2023.111.s8672.

[12] Lee D. W., Han J. S., Kim C. H., Ryu J. H., Song H. S., Lee Y. H., Experimental and Seepage Analysis of Gabion Retaining Wall Structure for Preventing Overtopping in Reservoir Dams, Applied Science, 14(10) 2024, pp. 1–14. https://doi.org/10.3390/app14104041.

[13] Chao M. T. T., Chueasamat A., Hori T., Saito H., Kohgo Y., Effectiveness of filter gabions against slope failure due to heavy rainfall, Soils and Foundations, 62(3), 2021, pp. 480-495. https://doi.org/10.1016/j.sandf.2021.01.010.

[14] Meng Y., Cu C., Yang Y., Li G., Wei X., Jia B., Seismic performance of reinforced soil slopes with gabions and geobags as slope facings in shaking table test, Vol. 198, 2025, pp. 1-15. https://doi.org/10.1016/j.soildyn.2025.109645.

[15] Kang M. W., Moon D. H., Roh H. -S., Jeon Y., Fu H., Lee S. S., Innovative upcycling gabions with coal bottom ash for nonpoint source pollution control against climate change, Journal of Cleaner Production, Vol. 478, 2024, pp. 1-12 https://doi.org/10.1016/j.jclepro.2024.143955.

[16] Wang Y., Smith J. V., Nazem M., Effect of Various Rainfall Conditions on the Roadside Stabilisation of Slopes in Gippsland, International Journal of Civil Engineering, 21(1), 2023, pp. 173–192. https://doi.org/10.1007/s40999-022-00752-x.

[17] Wang Y., Smith J. V., Nazem M., Optimisation of a Slope-Stabilisation System Combining Gabion-Faced Geogrid-Reinforced Retaining Wall with Embedded Piles, KSCE Journal of Civil Engineering, 25(12), 2021, pp. 4535–4551. https://doi.org/10.1007/s12205-021-1300-6.

[18] Filho J. A. P., Camelo D. G., Carvalho D. d., Dias A. G., Versolatto B. A. M., Use of

Construction and Demolition Solid Wastes for Basket Gabion Filling, Waste Management and Research: The Journla for a Sustainable Circular Economy, 38(12), 2020, pp. 1321–1330. https://doi.org/10.1177/0734242x20922591.

[19] Chakrabortty P., Srivastava L. S., Kumar P., A simple analytical model for bamboo-reinforced slopes using modified Bishop method, Frontiers in Built Environment, vol. 9, 2023, pp. 1-10. https://doi.org/10.3389/fbuil.2023.1080318.

[20] Ferren V., Magdalena I., Saengsupavanich C., Dhiya M. N. F., Sanitwong-Na-Ayuthaya S., Chandrasekan S., Solekhudin I., Azis M. I., Widowati, Analytical and Computational Methods for Optimizing Gabion-Pile Coastal Structures, Water, 17(4), 2025, pp. 1-18. https://doi.org/10.3390/w17040551.

[21] Wen J. Chu X., Xu L., Yu G., Li L., Probabilistic Pile Reinforced Slope Stability Analysis Using Load Transfer Factor Considering Anisotropy of Soil Cohesion, Engineering Reports, 6(6) 2024, pp. 1-15. https://doi.org/10.1002/eng2.12877.

[22] Wang Y., Nazem M., Smith J. V., Effect of Dimension Variables on the Behaviour of Slopes Stabilised by an Integrated Method Combining Gabion-Faced Geogrid-Reinforced Retaining Wall with Embedded Piles, International Journal of Geosynthethics and Groung Engineering, 8(65) 2022, pp. 1–19. https://doi.org/10.1007/s40891-022-00411-0.

[23] Chairullah B., Sungkar M., Munirwan R. P., Jamaluddin K., Ramadhani F. F., Jaya R. P., The Investigation of Stability on Slopes Utilizing Reinforcement Gabion wall and Concrete Piles for Mitigating Landslide Disasters, Open Construction and Building Technology Journal, 18(1), 2024, pp. 1-19. https://doi.org/10.2174/0118748368310059240605115115.

[24] Jaya L. M. G., Safani J., Okto A., Hasbi M., Kadir A., Ground deformation analysis on road infrastructure in north buton Indonesia using interferometric synthetic aperture radar (InSAR), IOP Conference Series: Earth and Environtmental Science, 419(1), 2020, pp. 1–6. https://doi.org/10.1088/1755-1315/419/1/012095.

[25] Badan Informasi Geospasial, "DEMNAS," 2018. https://tanahair.indonesia.go.id/demnas/#/demnas (accessed Mar. 07, 2024).

[26] Badan Standarisasi Nasional, SNI 19-6724-2002 Jaring Kontrol Horizontal. Jakarta: Badan Standarisasi Nasional, 2002, pp. 1-12.

[27] Ma J., Han Z., Liu F., Wang Z., Hu J., Zhang P., ConToGCN: A landslide susceptibility assessment model considering contour topographic features in slope units using graph convolution network, Catena, Vol. 255, 2025, pp. 1-26. https://doi.org/10.1016/j.catena.2025.109029.

[28] Zhou Y., Qi S. C., Fan G., Chen M. L., Zhou J. W., Topographic Effects on Three-Dimensional Slope Stability for Fluctuating Water Conditions Using Numerical Analysis, Water, 12(2), 2020, p. 1-24. https://doi.org/10.3390/W12020615.

[29] Nakileza B. R., Nedala S., Topographic influence on landslides characteristics and implication for risk management in upper Manafwa catchment, Mt Elgon Uganda, Geoenvironmental Disasters, 7(1), 2020, p. 1-13. https://doi.org/10.1186/s40677-020-00160-0.

[30] Setyawan A., Alina A., Suprapto D., Gernowo R., Suseno J. E., Hadiyanto H., Analysis slope stability based on physical properties in Cepoko Village, Indonesia, Cogent Engineering, 8(1), 2021, pp. 1–12. https://doi.org/10.1080/23311916.2021.1940637.

[31] Ullah R., Abdullah R. A., Kassim A., Yunus N. Z. M., Sendo H., Assessment Of Residual Soil Properties For Slope Stability Analysis, International Journal of GEOMATE, 21(86), 2021, pp. 72–80. https://doi.org/10.21660/2021.86.j2282.

[32] Habtemariam B. G., Shirago K. B., Dirate D. D., Effects of Soil Properties and Slope Angle on Deformation and Stability of Cut Slopes, Advances in Civil Engineering, Vol. 2022, 2022, pp. 1-10. https://doi.org/10.1155/2022/4882095.

[33] Badan Standarisasi Nasional, SNI 2878:2008 Cara Uji Penetrasi Lapangan dengan Alat Sondir. Jakarta: Badan Standarisasi Nasional, 2008, pp.1-28.

[34] Badan Standarisasi Nasional, SNI 2436:2008 Tata cara pencatatan dan identifikasi hasil pengeboran inti. Jakarta: Badan Standarisasi Nasional, 2008, pp. 1-141.

[35] Robertson P. K., Cone penetration test (CPT)-based soil behaviour type (SBT) classification system - an update, Canadian Geotechnical Journal, 53(12), 2016, pp. 1910–1927. https://doi.org/10.1139/cgj-2016-0044.

[36] Look B. G., Handbook of Geotechnical Investigation and Design Tables, 2nd Edition, London: CRC Press, 2017, pp. 67-157. https://doi.org/10.1201/b16520.

[37] Zhang, L. -M., Lu Q., Deng Z. -H., Zhang J., Probabilistic approach to determine rainfall thresholds for rainstorm-induced shallow landslides using long-term local precipitation records, Engineering Geology, Vol. 353, 2025, pp. 1-15. https://doi.org/10.1016/j.enggeo.2025.108139.

[38] Badan Standarisasi Nasional, SNI 3423:2008 Cara Uji Analisis Ukuran Butir Tanah. Jakarta: Badan Standarisasi Nasional, 2018, pp. 1-33.
[39] Badan Standarisasi Nasional, SNI 1743:2008 Cara Uji Kepadatan Berat Untuk Tanah. Bandung: Badan Standarisasi Nasional, 2008, pp. 1-14.
[40] Badan Standarisasi Nasional, SNI 1964:2008 Cara uji Berat Jenis Tanah. Jakarta: Badan Standarisasi Nasional, 2008, pp. 1-8.
[41] Badan Standardisasi Nasional, SNI 1965:2008 Cara Uji Penentuan Kadar Air untuk Tanah dan Batuan di Laboratorium. Jakarta: Badan Standarisasi Nasional, 2008, pp. 1-10.
[42] Badan Standardisasi Nasional, SNI 1966:2008 Cara Uji Penentuan Batas Plastis dan Indeks Plastisitas Tanah. Jakarta: Badan Standarisasi Nasional, 2008, pp. 1-8.
[43] Badan Standardisasi Nasional, SNI 1967:2008 Cara Uji Penentuan Batas Cair Tanah. Jakarta: Badan Standarisasi Nasional, 2008, pp. 1-18.
[44] Badan Standarisasi Nasional, SNI 3420:2016 Metode Uji Kuat Geser Langsung Tanah Terkonsolidasi dan Terdrainase. Jakarta: Badan Standarisasi Nasional, 2008, pp. 1-9.
[45] Li C., Zhao X., Xu X., Qu X., Study on the differences between Hoek–Brown parameters and equivalent Mohr–Coulomb parameters in the calculation slope critical acceleration and permanent displacement, Scientific Reports, 14(1), 2024, pp. 1–13. https://doi.org/10.1038/s41598-024-65494-3.
[46] Yang Y., Xia Y., Zheng H., Liu Z., Investigation of rock slope stability using a 3D nonlinear strength-reduction numerical manifold method, Engineering Geology, Vol. 292, 2021, pp. 1-15. https://doi.org//10.1016/j.enggeo.2021.106285.
[47] Renani H. R., Martin C. D., Factor of safety of strain-softening slopes, Journal of Rock Mechanics and Geotechnical Engineering, 12(3), 2020, pp. 473–483. https://doi.org/10.1016/j.jrmge.2019.11.004.
[48] Dyson A. P., Griffiths D. V., An efficient strength reduction method for finite element slope stability analysis, Computers and Geotechnics, Vol. 174, 2024, pp. 1-12. https://doi.org/10.1016/j.compgeo.2024.106593.
[49] Elsawwaf M. A. E., Azzam W. R., Kassem E. M., Behavior Of Reinforced Sand Slope With A Soft Pocket– Experimental And Numerical Study, International journal of GEOMATE, 22(94), 2022, pp. 47-58. https://doi.org/10.21660/2022.94.3170.
[50] Li P., Zhu C., Pan X., Lv B., Pan K., Undrained shear behavior of silty sand with a constant state parameter considering initial stress anisotropy effect, Scientific Reports, 14(2213), 2024, pp. 1–14. https://doi.org/10.1038/s41598-023-50901-y.
[51] Yang L., Yang F., Zhou Q., Zhang G., Research on Shear Strength Parameters of the Silty Fine Sand and the Rounded Gravel Layers in Nanning City, Advances in Civil Engineering, Vol. 2023, 2023, pp. 1-11. https://doi.org/10.1155/2023/7457038.
[52] Li Z., Mo S., Yang K., Chen Y., Coupled pore pressure analysis of cone penetration test in two-layered clay, Engineering Computations, 41(3), 2024, pp. 682–709. https://doi.org/10.1108/EC-10-2023-0721.
[53] American Society For Testing and Materials, ASTM D 2487-06 Standard Practice for Classification of Soils for Engineering Purposes (Unified Soil Classification System),. West Conshohocken, 2007, pp. 1-12.
[54] Chmielewski R., Bąk A., Muzolf P., Sobczyk K., Influence of Calculation Parameters on the Slope Stability of the Historical Rasos Cemetery in Vilnius (Lithuania), Sustainability, 16(7), 2024, pp. 1–16. https://doi.org/10.3390/su16072891.
[55] Dinh B. H., Nguyen A. D., Jang S. Y., Kim Y. S., Evaluation of erosion characteristics of soils using the pinhole test, International Journal of Geo-Engineering, 12(1), 2021, pp. 1–14. https://doi.org/10.1186/s40703-021-00145-4.
[56] Rasti A., Adarmanabadi H. R., Pineda M. C., Reinikainen J., Evaluating the Effect of Soil Particle Characterization on Internal Friction Angle, American Journal of Engineering and Applied Science, 14(1), 2021, pp. 129–138. https://doi.org/10.3844/ajeassp.2021.129.138.
[57] Badan Standarisasi Nasional, SNI 8460:2017 Persyaratan Perancangan Geoteknik. Jakarta: Badan Standarisasi Nasional, 2017.
[58] Wei S.-W., Lv S., Jiang J.-J., Cai D.-G., Cui Z.-D., Similarity Model Test on Rainfall Scouring Mechanism of High-Speed Railway Subgrade Slope, Applied Science, 14(1), 2023, pp. 1-15. https://doi.org/10.3390/app14010244.
[59] Wei S.-W., Cai D.-G., Lv S., Jiang J.-J., Cui Z.-D., Rainfall Scouring Mechanism of the High-Speed Railway Subgrade Slope with Coarse-Grained Soil, Advances in Civil Engineering, Vol. 2023, 2023, pp. 1–9. https://doi.org/10.1155/2023/7320049.